J|A|C|S
ARTICLES
Published on Web 12/14/2001

Synthesis and Characterization of Sulfur-Voided Cubanes. Structural Analogues for the $MoFe_3S_3$ Subunit in the Nitrogenase Cofactor

Dimitri Coucouvanis,*,† Jaehong Han,† and Namdoo Moon‡

Contribution from the Department of Chemistry and the Biophysics Research Division, The University of Michigan, Ann Arbor, Michigan 48109-1055

Received April 30, 2001

Abstract: A new class of Mo/Fe/S clusters with the $MoFe_3S_3$ core has been synthesized in attempts to model the FeMo-cofactor in nitrogenase. These clusters are obtained in reactions of the $(Cl_4\text{-cat})_2Mo_2Fe_6S_8(PR_3)_6$ [R = Et (**I**), ^{n}Pr (**II**)] clusters with CO. The new clusters include those preliminarily reported: $(Cl_4\text{-cat})MoFe_3S_3(PEt_3)_2(CO)_6$ (**III**), $(Cl_4\text{-cat})(O)MoFe_3S_3(PEt_3)_3(CO)_5$ (**IV**), $(Cl_4\text{-cat})(Pyr)MoFe_3S_3(PEt_3)_2(CO)_6$ (**VI**), and $(Cl_4\text{-cat})(Pyr)MoFe_3S_3(P^nPr_3)_3(CO)_4$ (**VIII**). In addition the new $(Cl_4\text{-cat})(O)MoFe_3S_3(P^nPr_3)_3(CO)_5$ cluster (**IVa**), the $(Cl_4\text{-cat})(O)MoFe_3S_3(PEt_3)_2(CO)_6$cluster (**V**), the $(Cl_4\text{-cat})(O)MoFe_3S_3(P^nPr_3)_2(CO)_6$ cluster (**Va**), the $(Cl_4\text{-cat})(Pyr)MoFe_3S_3(P^nPr_3)_2(CO)_6$ cluster (**VIa**), and the $(Cl_4\text{-cat})(P^nPr_3)MoFe_3S_3(P^nPr_3)_2(CO)_6$ cluster (**VII**) also are reported. Clusters **III**−**VIII** have been structurally and spectroscopically characterized. EPR, zero-field ^{57}Fe-Mössbauer spectroscopic characterizations, and magnetic susceptibility measurements have been used for a tentative assignment of the electronic and oxidation states of the $MoFe_3S_3$ sulfur-voided cuboidal clusters. A structural comparison of the clusters with the $MoFe_3S_3$ subunit of the FeMo-cofactor has led to the suggestion that the storage of reducing equivalents into M−M bonds, and their use in the reduction of substrates, may occur with the FeMo-cofactor, which also appears to have M−M bonding. On the basis of this argument, a possible N_2-binding and reduction mechanism on the FeMoco-cofactor is proposed.

Introduction

Nitrogen fixation, one of the fundamental reactions in nature, is carried out by nitrogenase. The enzyme is a complex of two proteins,[1] the Fe protein (60 kD) and the MoFe protein (240 kD). Of these the former transfers electrons to the latter where reduction of dinitrogen to ammonia occurs. The Fe protein has a $[Fe_4S_4]$-type Fe/S cluster between two units of a homodimer. The MoFe protein, $\alpha_2\beta_2$ tetramer has two different types of inorganic clusters. These clusters are the P cluster (Fe_8S_7) and the FeMo-cofactor, FeMoco, (*R*-homocitrate-$MoFe_7S_9$) (Figure 1). The P cluster is believed to accept electrons from the Fe protein and transfers these electrons to the FeMoco eventually where activation and reduction of N_2 is thought to take place.[2] During the two-electron redox cycle, the P cluster undergoes a significant structural change between two oxidation states, P^N and P^{OX} (Figure 1).[1(b),3]

Although the mechanism of nitrogenase action has been investigated extensively[4] and the structure of the FeMoco is known to high resolution,[1c] there still remain fundamental questions that need to be answered. Of particular interest are questions concerning the site of activation and reduction of dinitrogen and structural changes that may accompany the reduction of the cofactor to the N_2 reducing state. The former of these questions has been addressed on numerous occasions and many speculations concerning nitrogen activation have been advanced. Most of these are based on theoretical calculations at various levels of sophistication.[5]

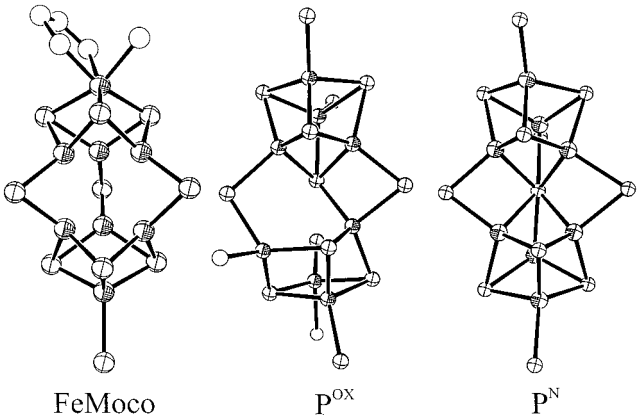

Figure 1. Structure of the FeMoco and the P clusters.[1c] The P^N cluster is the two-electron reduced form of the P^{OX} cluster. The spheres with octant shading represent Fe atoms and those without shading represent S atoms. Terminal carbon, nitrogen, and oxygen ligands are shown as simple spheres.

† Department of Chemistry.
‡ Biophysics Research Division.

(1) (a) Howard, J. B.; Rees, D. C. *Chem. Rev.* **1996**, *96*, 2965 and references therein. (b) Peters, J. W.; Stowell, M. H. B.; Soltis, S. M.; Finnegan, M. G.; Johnson, M. K.; Rees, D. C. *Biochemistry* **1997**, *36*, 1181. (c) Mayer, S. M.; Lawson, D. M.; Gormal, C. A.; Roe, S. M.; Smith, B. E. *J. Mol. Biol.* **1999**, *292*, 871.
(2) (a) Lanzilotta, W. N.; Seefeldt, L. C. *Biochemistry* **1996**, *35*, 16770. (b) Lanzilotta, W. N.; Fisher, K.; Seefeldt, L. C. *Biochemistry* **1996**, *35*, 7188. (c) Shah, V. K.; Brill, W. J. *Proc. Natl. Acad. Sci. U.S.A.* **1977**, *74*, 3249.
(3) Musgrave, K. B.; Liu, H. I.; Ma, L.; Burgess, B. K.; Watt, G.; Hedman, B.; Hodgson, K. O. *J. Biol. Inorg. Chem.* **1998**, *3*, 344.
(4) Burgess, B. K.; Lowe, D. J. *Chem. Rev.* **1996**, *96*, 2983.

10.1021/ja0110832 CCC: $22.00

The unusual structure of the FeMoco apparently is retained following extraction from the MoFe protein by NMF [6] or pyrolidinone. This isolated FeMoco can be reincorporated into the inactive apoprotein to restore the function. Various studies on the isolated FeMoco have provided mechanistic insights regarding catalysis as well as understanding its electronic and physical properties.[7]

The nitrogenase FeMoco consists of two cuboidal cluster subunits ($MoFe_3S_3$ and Fe_4S_3) connected by μ_2-bridging inorganic sulfido ligands. The apparent coordination unsaturation of the six inner Fe atoms initially was the cause of considerable excitement and speculation. The more recent, high-resolution structures of the MoFe protein of nitrogenase,[1b,c] however, indicate very short Fe−Fe inter- and intra-subunit distances and reveal Fe−Fe bonding as an important structural feature. If metal−metal bonds are indeed important in the structure of the FeMoco core, the apparent three-coordinate iron sites in the cofactor could also be described as coordinatively saturated six- or seven-coordinate iron sites (Figure 1).

We have shown that the $(Cl_4\text{-cat})_2Mo_2Fe_6S_8(PR_3)_6$ [R = Et (**I**), ^{n}Pr (**II**), ^{n}Bu][8] clusters that can be synthesized from simple $(Et_4N)_2[(Cl_4\text{-cat})MoOFeS_2Cl_2]$ and $(Et_4N)_2[Fe_2S_2Cl_4]$ building blocks by a reductive coupling reaction[9] are highly reactive molecules. The $(Cl_4\text{-cat})_2Mo_2Fe_6S_8(PEt_3)_6$ (**I**) cluster, and the P^nPr_3 or P^nBu_3 analogues show relatively strong M−M interactions and the $[MoFe_3S_4]$ subunits are one-electron reduced by comparison to "conventional" Mo/Fe/S clusters. Under reducing conditions, **I** affords $[(Cl_4\text{-cat})_2Mo_2Fe_6S_8(PEt_3)_6]^{4-}$. In this cluster,[10] two Fe atoms have FeS_3 trigonal planar coordination geometry, similar to that found in the FeMoco prismatic Fe center.

Reductive desulfurization of either $(Cl_4\text{-cat})_2Mo_2Fe_6S_8(PEt_3)_6$ (**I**)[11] or $(Cl_4\text{-cat})_2Mo_2Fe_6S_8(P^nPr_3)_6$ (**II**)[12] under moderate CO pressures affords new clusters with $[MoFe_3S_3]$ cores with terminally coordinated CO and PR_3 and Mo-bound Cl_4-cat ligands. These clusters structurally resemble the Mo-containing cuboidal subunit of the FeMoco and their structural features (particularly metal−metal distances) have been discussed with respect to the total valence electron count in the clusters.[12]

In this paper we report in detail the synthesis, structural characterization, physical and spectroscopic properties, and chemical reactivity of the new Roussin-type compounds, $(Cl_4\text{-cat})(O)MoFe_3S_3(P^nPr_3)_3(CO)_5$ (**IIIa**), $(Cl_4\text{-cat})(O)MoFe_3S_3(P^nPr_3)_2(CO)_6$ (**Va**), $(Cl_4\text{-cat})(Pyr)MoFe_3S_3(P^nPr_3)_2(CO)_6$ (**VIa**), and $(Cl_4\text{-cat})(P^nPr_3)MoFe_3S_3(P^nPr_3)_2(CO)_6$ (**VII**), as well as the previously reported[11,12] $(Cl_4\text{-cat})MoFe_3S_3(PEt_3)_2(CO)_6$ (**III**), $(Cl_4\text{-cat})(O)MoFe_3S_3(PEt_3)_3(CO)_5$ (**IV**), $(Cl_4\text{-cat})Mo(O)Fe_3S_3(PEt_3)_2(CO)_6$ (**V**), $(Cl_4\text{-cat})(Pyr)MoFe_3S_3(PEt_3)_2(CO)_6$ (**VI**), and $(Cl_4\text{-cat})(Pyr)MoFe_3S_3(P^nPr_3)_3(CO)_4$ (**VIII**) clusters. Studies on these synthetic clusters (Figure 2), partial analogues of the FeMoco, have provided fundamental information that may be useful in understanding the structure and function of the FeMoco in nitrogenase.

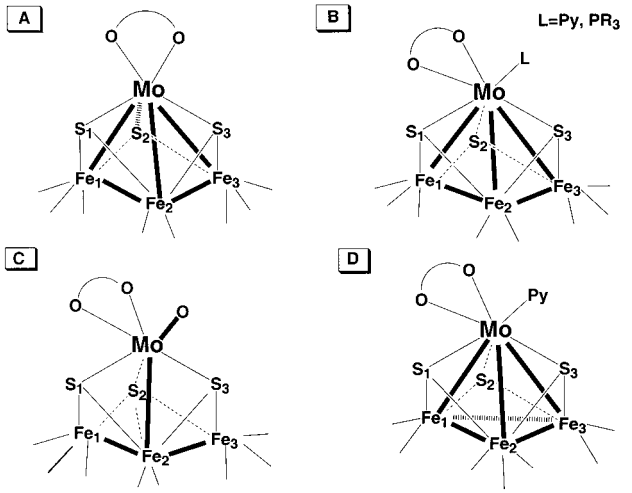

Figure 2. Schematic structures and labeling of the $[MoFe_3S_3]$ Roussin-type compounds: (A) $(Cl_4\text{-cat})MoFe_3S_3(PEt_3)_2(CO)_6$ (**III**); (B) $(Cl_4\text{-cat})(Pyr)MoFe_3S_3(PEt_3)_2(CO)_6$ (**VI**), $(Cl_4\text{-cat})(Pyr)MoFe_3S_3(P^nPr_3)_2(CO)_6$ (**VIa**), and $(Cl_4\text{-cat})(P^nPr_3)MoFe_3S_3(P^nPr_3)_2(CO)_6$ (**VII**); (C) $(Cl_4\text{-cat})(O)MoFe_3S_3(PEt_3)_3(CO)_5$ (**IV**), $(Cl_4\text{-cat})(O)MoFe_3S_3(P^nPr_3)_3(CO)_5$ (**IVa**), $(Cl_4\text{-cat})(O)MoFe_3S_3(PEt_3)_2(CO)_6$ (**V**), and $(Cl_4\text{-cat})(O)MoFe_3S_3(P^nPr_3)_2(CO)_6$ (**Va**); and (D) $(Cl_4\text{-cat})(Pyr)MoFe_3S_3(P^nPr_3)_3(CO)_4$ (**VIII**).

Experimental Section

General. All experiments and reactions were carried out under a dinitrogen atmosphere with standard Schlenk line techniques or in an inert atmosphere glovebox. All solvents were distilled under dinitrogen and nitrogen gas was bubbled through each before use in the glovebox. Acetonitrile was predried over oven-dried molecular sieves and distilled over CaH_2. Ethyl ether and THF were predried over Na ribbon and further purified by the Sodium-Benzoketyl method. Dichloromethane was distilled over P_2O_5. $FeCl_2$, PEt_3, and P^nPr_3 were purchased from STREM and used for the reaction without further purification. CO (99.9%) was purchased from Matheson Gas and used with the O_2 trap installed. $(Cl_4\text{-cat})_2Mo_2Fe_6S_8(PEt_3)_6$ (**I**) and $(Cl_4\text{-cat})_2Mo_2Fe_6S_8(P^nPr_3)_6$ (**II**) were synthesized according to published methods.[9,12,13]

FT-IR spectra were collected on a Nicolet DX V. 4.56 FT-IR spectrometer in KBr pellets and the spectra were corrected for background. Elemental analyses were performed by the Microanalytical Laboratory at the University of Michigan. The data were adjusted by using acetanilide as a standard. Electronic spectra were recorded on a Varian CARY 1E UV−visible spectrometer. Cyclic voltammetry experiments were carried out by a EG & G M260 potentiostat with use of a Pt working electrode, unless otherwise indicated. The potentials are reported vs Ag/AgCl as a reference electrode with use of 0.1 M of $(^nBu_4N)(PF_6)$ as supporting electrolyte. Mössbauer spectra were obtained with the high-sensitivity Mössbauer spectrometer in the Biophysics department at the University of Michigan.[14] All the Mössbauer measurements were carried out at 125 K in zero applied magnetic field. The source was ^{57}Co in a Rh matrix and the isomer shift was reported versus Fe metal at room temperature. The magnetic susceptibility measurements were carried out on a MPMS SQUID magnetometer and the data were corrected for diamagnetic contributions. FAB^+ mass spectra were obtained at the University of Michigan Mass Spectroscopy Laboratory with a 3-nitrobenzoyl alcohol matrix.

(5) (a) Dance, I. *Chem. Commun*. **1988**, 523. (b) Dance, I. *Chem. Commun*. **1997**. 165. (c) Dance, I. *J. Biol. Inorg. Chem.* **1997**, *1*, 165. (d) Barriere, F.; Pickett, C. J.; Talarmin, J. *Polyhedron* **2001**, *20*, 27. (e) Stavrev, K. K.; Zerner, M. C. *Int. J. Quantum Chem*. **1998**, *70*, 1159. (f) Durrant, M. C. *Inorg. Chem. Commun*. **2001**, *4*, 60.
(6) *N*-Methylformamide.
(7) Smith, B. E.; Durrant, M. C.; Fairhurst, S. A.; Gormal, C. A.; Grönberg, K. L. C.; Henderson, R. A.; Ibrahim, S. K.; Le Gall, T.; Pickett, C. J. *Coord. Chem. Rev*. **1999**, *185*−*186*, 669.
(8) Cl_4-cat = tetrachlorocatecholate.
(9) Han, J.; Koutmos, M.; Al-Ahmad, S.; Coucouvanis, D. *Inorg. Chem.* **2001**, *40*, 5985.
(10) Osterloh, F.; Achim, C.; Holm, R. H. *Inorg. Chem*. **2001**, *40*, 224.
(11) Tyson, M. A.; Coucouvanis, D. *Inorg. Chem.* **1997**, *36*, 3808.
(12) Han, J.; Beck, K.; Ockwig, N.; Coucouvanis, D. *J. Am. Chem. Soc*. **1999**, *121*, 10448.
(13) Demadis, K. D.; Campana, C. F.; Coucouvanis, D. *J. Am. Chem. Soc*. **1995**, *117*, 7832.
(14) Moon, N.; Coffin, C. T.; Steinke, D. C.; Sands, R. H.; Dunham, W. R. *Nucl. Inst. Methods Phys. Res. B* **1996**, *119*, 555.

Schematic structures of the compounds are shown in Figure 2 and their identifying numbers are as follows: $(Cl_4\text{-cat})_2Mo_2Fe_6S_8(PEt_3)_6$ (**I**); $(Cl_4\text{-cat})_2Mo_2Fe_6S_8(P^nPr_3)_6$ (**II**); $(Cl_4\text{-cat})MoFe_3S_3(PEt_3)_2(CO)_6$ (**III**); $(Cl_4\text{-cat})(O)MoFe_3S_3(PEt_3)_3(CO)_5$ (**IV**); $(Cl_4\text{-cat})(O)MoFe_3S_3(P^nPr_3)_3(CO)_5$ (**IVa**); $(Cl_4\text{-cat})(O)MoFe_3S_3(PEt_3)_2(CO)_6$ (**V**); $(Cl_4\text{-cat})(O)MoFe_3S_3(P^nPr_3)_2(CO)_6$ (**Va**); $(Cl_4\text{-cat})(Pyr)MoFe_3S_3(PEt_3)_2(CO)_6$ (**VI**); $(Cl_4\text{-cat})(Pyr)MoFe_3S_3(P^nPr_3)_2(CO)_6$ (**VIa**); $(Cl_4\text{-cat})(P^nPr_3)MoFe_3S_3(P^nPr_3)_2(CO)_6$ (**VII**); and $(Cl_4\text{-cat})(Pyr)MoFe_3S_3(P^nPr_3)_3(CO)_4$ (**VIII**).

Carbonylation Products of $(Cl_4\text{-cat})_2Mo_2Fe_6S_8(PEt_3)_6$ (I). The $(Cl_4\text{-cat})_2Mo_2Fe_6S_8(PEt_3)_6$ cluster (**I**) (1.0 g, 0.504 mmol) was dissolved in CH_2Cl_2 (50 mL) and the solution was put into the high-pressure reactor. CO gas (500psi) was introduced and the reaction mixture was stirred for 3 days. The reaction mixture had undergone a change in color to reddish black from the greenish black color of the starting material. The CO was vented by releasing pressure and the solvent was removed by nitrogen purging. The residue was isolated with flash column chromatography using hexanes and CH_2Cl_2 eluents on TLC [15] silica gel. The reaction products from each fraction have been crystallized and identified by FT-IR spectroscopy. Four products were isolated: **III**, **IV**, **V**, and **VI**.

$(Cl_4\text{-cat})MoFe_3S_3(PEt_3)_2(CO)_6$ (III): $R_f = 0.58$ (CH_2Cl_2:Hexanes = 1:1), 20−50% yield. FT-IR (KBr, cm^{-1}) 2974 (w), 2965 (w), 2938 (w), 2880 (w), 2025 (vs), 2002 (s), 1977 (vs), 1960 (s), 1937 (s), 1900 (m), 1412 (s), 1036 (m), 984 (m), 811 (w), 789 (w), 761 (w), 414 (s), 379 (w), 333 (m). ^{1}H NMR (CD_2Cl_2, 400 MHz) 1.95 (m, CH_2, 12H), 1.19 (m, CH_3, 18H). UV−vis (CH_2Cl_2, nm) 309, 471. Magnetic susceptibility: 3.68 μ_B (300 K), 0.64 μ_B (4 K). EPR (frozen CH_2Cl_2) silent.

$(Cl_4\text{-cat})(O)MoFe_3S_3(PEt_3)_3(CO)_5$ (IV): $R_f = 0.73$ (CH_2Cl_2:Hexanes = 1:1), 0−50% yield. Compound **IV** also can be isolated from the reaction mixture of $(Et_4N)_2[(Cl_4\text{-cat})(MeCN)MoFe_3S_4Cl_3]$ and high-pressure CO. FT-IR (KBr, cm^{-1}) 2966 (w), 2937 (w), 2909 (w), 2880 (w), 2022 (vs), 1989 (s), 1974 (s), 1959 (s), 1893 (m), 1428 (s), 1033 (m), 980 (m), 928 (m, $\nu_{Mo=O}$), 811 (w), 765 (w), 474 (m), 427 (m), 411 (m), 377 (s), 346 (m), 333 (s), 312 (m), 278 (m). ^{1}H NMR ($CDCl_3$, 400 MHz) 2.08 (6H, m), 1.80 (6H, q, $J = 8.0$), 1.62 (6H, q, $J = 8.0$), 1.19 (9H, t, $J = 8.0$), 1.13 (9H, t, $J = 8.0$), 1.02 (9H, t, $J = 8.0$). FAB^+-MS (NBA as matrix, *m/z*)[16] 1117 ($[M + H^+]^+$, 1.87), 1061 (0.44), 1032 (1.11), 1004 (1.30), 976 (base peak), 858 (27.40), 740 (12.09). UV−vis (CH_2Cl_2, nm) 312 (sh). Magnetic susceptibility: 1.01 μ_B (300 K), 0.39 μ_B (4 K). EPR (frozen CH_2Cl_2) silent.

$(Cl_4\text{-cat})(O)MoFe_3S_3(PEt_3)_2(CO)_6$ (V): $R_f = 0.82$ (CH_2Cl_2:Hexanes = 1:1), ca. 12% yield. Compound **V** was also synthesized by reacting **III** with dibenzyl trisulfide or trimethyl-*N*-oxide.

(a) Reaction of III with dibenzyl trisulfide: Compound **III** (200 mg) was dissolved in THF or toluene and dibenzyl trisulfide was added into the solution. When the IR showed no starting material, the reaction mixture was crystallized by the hexane diffusion. The aimed product was isolated as crystalline material in 50% yield. FT-IR (KBr, cm^{-1}) 2972 (w), 2937 (w), 2880 (w), 2043 (vs), 2034 (s), 2019 (s), 1997 (vs), 1980 (s), 1966 (s), 1943 (m), 1424 (s), 1378 (m), 1248 (m), 1033 (m), 982 (m), 936 (m, $\nu_{Mo=O}$), 813 (m), 763 (m), 577 (m), 538 (m), 472 (m), 464 (m), 429 (m), 362 (w), 350 (s), 343 (s), 310 (m), 300 (s). ^{1}H NMR (300 MHz,C_6D_6) 1.60−1.71 (m, 6H), 1.33−1.44 (m, 6H), 0.57 (d of t, $J = 17$ Hz, 8 Hz, 18H). Anal. Calcd for $MoFe_3Cl_4S_3P_2O_9C_{24}H_{30}\cdot 5CH_2Cl_2$ (MW 1025.92): C, 24.01; H, 2.78. Found: C, 24.18; H, 2.74. UV−vis (CH_2Cl_2, nm) 325, 445. EPR (frozen CH_2Cl_2) silent.

(b) Reaction of III with trimethyl-N-oxide: To a solution of **III** (170 mg; 0.141 mmol) in 20 mL of CH_2Cl_2 was added trimethyl-*N*-oxide (21.2 mg; 0.282 mmol). The reaction mixture was stirred at room temperature and monitored by IR spectroscopy. The reaction was terminated when all **III** was consumed. Column chromatography (silica gel; eluent: 20% CH_2Cl_2 in hexane) gave the desired product **V** as a black solid in 30% yield.

$(Cl_4\text{-cat})(Pyr)MoFe_3S_3(PEt_3)_2(CO)_6$ (VI): ca. 25% yield. This compound isolated when the reaction mixture contained an extra 1 mL of pyridine in CH_2Cl_2. FT-IR (KBr, cm^{-1}) 2975 (w), 2965 (w), 2936 (m), 2909 (w), 2879 (w), 2026 (s), 2005 (s), 1975 (s), 1945 (vs), 1891 (m) 1443 (s), 1258 (m), 1038 (m), 1033 (m), 978 (m), 807 (m), 781 (m), 755 (m), 693 (w), 441 (s), 430 (s), 412 (s), 351 (w), 354 (m), 327 (w), 302 (s); FT-IR (CH_2Cl_2, cm^{-1}) ν_{CO} (2025, 1998, 1978, 1957). ^{1}H NMR (400 MHz, CD_2Cl_2)[17] 8.21 (br s, 2H), 7.20 (br s, 1H), 6.80 (br s, 2H), 1.992 (m, 8H), 1.261 (br s, 6H), 1.247 (br s, 3H), 1.206 (t, $J = 8$, 9H), 1.144 (m, 4H). UV−vis (CH_2Cl_2, nm) 322, 424. Magnetic susceptibility: 1.61 μ_B (300 K), 1.19 μ_B (4.19 K). EPR (frozen CH_2Cl_2) silent.

Carbonylation Products of $(Cl_4\text{-cat})_2Mo_2Fe_6S_8(P^nPr_3)_6$ (II). The $(Cl_4\text{-cat})_2Mo_2Fe_6S_8(P^nPr_3)_6$ cluster (**II**) (1.0 g, 0.447 mmol) in CH_2Cl_2 (50 mL) was used for the carbonylation reaction. The residue was isolated with flash column chromatography using *n*-pentane, hexanes, and CH_2Cl_2 eluents on TLC silica gel. The reaction products have been crystallized from each fraction and identified by FT-IR. Five products were chromatographically separated and isolated.

$(Cl_4\text{-cat})(O)MoFe_3S_3(P^nPr_3)_3(CO)_5$ (IVa): $R_f = 0.79$ (CH_2Cl_2:Hexanes = 1:1), ca. 10% yield. FT-IR (KBr, cm^{-1}) 2963 (m), 2930 (w), 2871 (w), 2018 (vs), 1995 (s, sh), 1988 (s), 1960 (s), 1948 (m), 1892 (m), 1429 (s), 1249 (w), 1076 (m), 982 (m), 947 (m, $\nu_{Mo=O}$), 811 (m), 572 (w), 475 (w), 431 (w), 377 (m), 368 (m), 361 (m sh). Anal. Calcd for $MoFe_3Cl_4S_3P_3O_8C_{38}H_{63}\cdot CH_2Cl_2$ (MW 1327.239): C, 35.29; H, 4.94. Found: C, 35.21; H,4.87. EPR (frozen CH_2Cl_2) silent.

$(Cl_4\text{-cat})(O)MoFe_3S_3(P^nPr_3)_2(CO)_6$ (Va): $R_f = 0.84$ (CH_2Cl_2:Hexanes = 1:1), ca. 10% yield. FT-IR (KBr, cm^{-1}) 2963 (m), 2931 (w), 2872 (w), 2044 (vs), 2026 (s), 2009 (vs), 1986 (vs), 1981 (s, sh), 1951 (s), 1936 (m), 1423 (s), 1248 (m), 1076 (m), 982 (m), 940 (m, $\nu_{Mo=O}$), 812 (m), 788 (m), 576 (m), 538 (m), 488 (m), 430 (m), 407 (w), 376 (m), 322 (m). EPR (frozen CH_2Cl_2) silent. FAB^+-MS (NBA as matrix, *m/z*) 1111.0 ($[M + H]^+$, 3.74), 1078.9 (2.04), 1062.9 (11.37), 957.9 ($[M - P^nPr_3]^+$, 12.08), 941.9 (base peak). Anal. Calcd for $MoFe_3Cl_4S_3P_2O_9C_{30}H_{42}\cdot {}^1/_2$Hex (MW 1153.168): C, 34.37; H, 4.28. Found: C, 34.88; H, 4.56.

$(Cl_4\text{-cat})(P^nPr_3)MoFe_3S_3(P^nPr_3)_2(CO)_6$ (VII): $R_f = 0.87$ (CH_2Cl_2:Hexanes = 1:1), ca. 20% yield. IR (KBr, cm^{-1}) 2963 (m), 2930 (w), 2872 (w) 2022 (vs), 1987 (vs), 1974 (s), 1958 (s), 1928 (s), 1873 (m), 1423 (s), 1251 (m), 1078 (m), 976 (m), 810 (w), 783 (w), 543 (m), 426 (s), 414 (s), 401 (sh), 335 (m). FAB^+-MS (NBA as matrix, *m/z*) 1421.4 ($[M + NBA]^+$), 1403.4 ($[1241.4 - CO]^+$), 1241.3 ($[1403.4 - P^nPr_3]^+$), 1062.9 ($[M - (P^nPr_3 + CO)]^+$). UV−vis (CH_2Cl_2, nm) 319, 439 (sh), 588 (sh).

$(Cl_4\text{-cat})(Pyr)MoFe_3S_3(P^nPr_3)_2(CO)_6$ (VIa): $R_f = 0.74$ (CH_2Cl_2:Hexanes = 1:1), ca. 30% yield. This compound and **VIII** were isolated when the reaction mixture contained an extra 1 mL of pyridine in CH_2Cl_2. IR(KBr, cm^{-1}) 2961 (m), 2929 (w), 2870 (w) 2017 (vs), 1986 (vs), 1973 (m), 1968 (m), 1949 (sh), 1940 (s), 1873 (m), 1419 (s), 1257 (m), 1074 (m), 977 (m), 809 (m), 786 (w), 551 (m), 542 (m). ^{1}H NMR (400 MHz, CD_2Cl_2) 1.92 (m, 12H), 1.61 (m, 12H), 1.07 (t, $J = 6.5$, 18H). Absorption spectrum (CH_2Cl_2) λ_{max}, 322 nm, 450 nm (sh), 580 nm (sh). Anal. Calcd for $MoFe_3Cl_4S_3P_2NO_8C_{35}H_{47}$ (MW 1173.181): C, 35.83; H, 4.04; N, 1.19. Found: C, 35.74; H, 4.06; N, 1.19. Magnetic susceptibility: 0.65 μ_B (300 K), 1.19 μ_B (25 K), 1.10 μ_B (4 K). EPR (frozen CH_2Cl_2) silent.

$(Cl_4\text{-cat})(Pyr)MoFe_3S_3(P^nPr_3)_3(CO)_4$, (VIII): $R_f = 0.77$ (CH_2Cl_2:Hexanes = 1:1), ca. 9% yield. Black rhombic crystals. FT-IR (KBr, cm^{-1}) 2963 (s), 2930 (m), 2872 (w), 2021 (vs), 1987 (vs), 1974 (m),

(15) TLC = thin-layer chromatography.
(16) The isotope distributions at molecular ion peak correspond well to the calculated pattern. Removal of PEt_3 and CO was observed from *m/z* 976, 858, and 740 peaks, and from *m/z* =1061, 1032, and 1004 peaks, respectively.
(17) The sample converts to **V** over a day in the NMR tube like **III**, which was observed from NMR spectra.

1958 (s), 1928 (s), 1425 (s), 1259 (m), 810 (m), 796 (m), 565 (w), 542 (w), 518 (s), 476 (s), 407 (m), 398 (m), 328 (m). ^{1}H NMR (400 MHz, CD_2Cl_2) 1.89 (br s, 18H), 1.74 (m, 18H), 1.60 (m, 27H). Absorption spectrum (CH_2Cl_2) λ_{max}, 313 nm. FAB$^+$-MS (FAB$^+$ in NBA w/Na$^+$; *m*/*z*, relative intensity) 1101.5 (5.0, [M − P^{n}Pr$_3$]$^+$), 941.6 (9.6, [M − 2(P^{n}Pr$_3$)]$^+$). EPR (frozen CH_2Cl_2) silent.

X-ray Crystallography. The crystals isolated from the chromatographic fractions were attached to glass fibers and diffraction data were collected at 158(2) K with a Siemens SMART area diffractometer. Absorption corrections have not been applied to the data. The crystal data and structural parameters for compounds **IVa**, **Va**, **VIa**, and **VII** have been deposited. The structures were solved by direct methods to locate heavy atoms and the non-hydrogen atoms were located through subsequent difference Fourier syntheses. Structural refinements were carried out by full-matrix least-squares on F∧2. Hydrogen atoms were assigned idealized positions. All non-hydrogen atoms were refined with anisotropic thermal parameters and all hydrogen atoms were refined isotropically. All calculations were performed with SHELXTL-NT V. 5.1 software.

Results and Discussion

Synthesis. Since the original synthesis of the $(Cl_4\text{-cat})_2Mo_2Fe_6S_8(PEt_3)_6$, edge-fused double cubane (**I**),[13] the anticipated reactivity of this interesting molecule has been demonstrated[18] and is still being explored by us[11,12] and others.[10,19] Interest in **I** derives from a core stoichiometry (M_8S_8) close to that of the nitrogenase cofactor (M_8S_9) and an average Fe oxidation state also close to that of the FeMoco.

The $[MoFe_3S_4]^{2+}$ cuboidal subunits in **I** are reduced by one electron relative to the known[20] $[MoFe_3S_4]^{3+}$ clusters and show shorter Fe−Fe and Fe−Mo distances. The latter at 2.639(3) and 2.677(5) Å, respectively, are quite similar to corresponding distances determined by EXAFS data analysis for the nitrogenase cofactor.[21] The high-resolution structures of the MoFe proteins from *Azotobacter vinelandii*[1b] and *Klebsiella pneumoniae*[1c] have revealed the structure of FeMoco to nearly atomic resolution (Figure 1). They clearly show unusually short Fe−Fe and Mo−Fe distances and strongly suggest that M−M bonding is an important structural feature of FeMoco. As a result, each of the iron atoms within the central Fe_6, trigonal prismatic array appears to be bound to four other neighboring metal atoms (Figure 1). The six FeS_3 units within the Fe_6 array originally were described as coordinatively unsaturated Fe sites;[22] however, it is also likely that metal−metal interactions provide additional coordination and enough electron density to satisfy the electron count needed for the FeS_3 units.

In search of new, reduced clusters with pronounced M−M bonding interactions, we have explored the reactivity of **I** and **II** with CO. Previous, similar reactivity studies with the $[Fe_4S_4(SPh)_4]^{2-}$ cluster have been reported to afford products that contain CO ligands.[23]

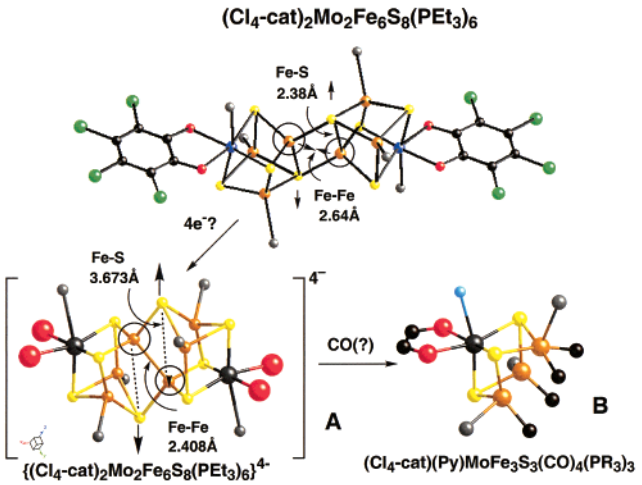

Figure 3. Proposed formation of the $[(Cl_4\text{-cat})_2Mo_2Fe_6S_8(PEt_3)_6]^{4-}$ cluster **A** by reduction of the $(Cl_4\text{-cat})_2Mo_2Fe_6S_8(PEt_3)_6$ cluster (**I**).[10] The subunits in **A** are compared to the $(Cl_4\text{-cat})(Pyr)MoFe_3S_3(PR_3)_3(CO)_4$ cluster **B** obtained[12] by a CO reaction with **I**.

The reaction of **I** with CO, at a moderate pressure of 500 psi, results in a multitude of CO containing products. A common feature in most of these products (**III**, **IV**, **V**, and **VI**, Table 1 and Figure 2) is a $[MoFe_3S_3]^{2+}$ core with the iron atoms collectively reduced by two electrons when compared with the $[MoFe_3S_4]^{2+}$ cores in **I**. The reaction of **II** with CO affords similar products with the same core structure (**IVa**, **Va**, **VIa**, **VII**, and **VIII**) but in different relative amounts. The core reduction in **I**, that probably precedes formation of the $[MoFe_3S_3]^{2+}$ units, very likely is brought about by the PR_3 ligands which, by oxidative S^{2-} abstraction from the cubic subunits in **I** and **II**, generate S═PR$_3$ and the $[MoFe_3S_3]^{2+}$ units. The latter are quite rare in M/S chemistry, and structurally similar variants exist only in the $[Fe_4S_3(NO)_7]^+$ "Roussin" salt[24] and its PR_3 derivatives.[25] A pathway to the formation of the new, $[MoFe_3S_3]^{2+}$ containing clusters can be envisioned in terms of a structural rearrangement of **I** or **II**, to a cofactor-like $[Mo_2Fe_6S_8(L)_4]$ cluster prior to or following reduction and reaction with CO (Scheme 1). Indeed a rearrangement of **I**, following reduction, is apparent in a recently reported new cluster[10] (Figure 3). Whether this new cluster (**A**) will react with CO to give a cluster similar to **VIII** (Figure 3B) remains to be established. The structure of this centrosymmetric molecule (**I**$^{4-}$, Figure 3A) shows an unusually short Fe−Fe distance between the two $MoFe_3S_3$ subunits and two planar FeS_3 sites very much like those found in the FeMoco.

The cores of the individual subunits in **I**$^{4-}$ are structurally and electronically nearly identical to **VIII** (same formal oxidation states for the Fe and Mo atoms and a Roussin-type of structure). They are obtained by breaking two of the Fe−S edges in the rhombic Fe_2S_2 bridge in **I**. The resulting new structure now consists of two $MoFe_3S_3$ subunits bridged by two S^{2-} ligands (Figure 3A).

The driving force for the structural rearrangement of **I** or **II** (Scheme 1) and formation of the $MoFe_3S_3$ clusters could be the possibly greater thermodynamic stability of the Roussin-

(18) Demadis, K. D. Thesis, University of Michigan, 1995.
(19) (a) Osterloh, F.; Segal, B. M.; Achim. C.; Holm, R. H. *Inorg. Chem*. **2000**, *39*, 980. (b) Osterloh, F.; Sanakis, Y.; Staples, R. J.; Münck, E.; Holm, R. H. *Angew. Chem., Int. Ed*. **1999**, *38*, 2066.
(20) (a) Malinak, S. M.; Coucouvanis, D. *Prog. Inorg. Chem*. **2001**, *49*, 599. (b) Coucouvanis, D. *ACS Sym. Ser*.**1993**, *535*, 304. (c) Holm, R. H.; Simhon, E. D. In *Molybdenum Enzymes*; Spiro, T. G., Ed.; Wiley-Interscience: New York, 1985; pp 1−87.
(21) (a) Christiansen, J.; Tittsworth, R. C.; Hales, B. J.; Cramer, S. P. *J. Am. Chem. Soc*. **1995**, *117*, 10017. (b) Liu, H. B. I.; Filipponi, A.; Gavini, N.; Burgess, B. K.; Hedman, B.; Dicicco, A.; Natoli, C. R.; Hodgson, K. O. *J. Am. Chem. Soc*. **1994**, *116*, 2418. (c) Chen, J.; Christiansen, J.; Titsworth, R. C.; Hales, B. J.; Cramer, S. P. *J. Am. Chem. Soc*. **1993**, *115*, 5509. (d) Conradson, S. D.; Burgess, B. K.; Newton, W. E.; Mortenson, L. E.; Hodgson, K. O. *J. Am. Chem. Soc*. **1987**, *109*, 7507.
(22) Kim, J.; Rees, D. C. *Science* **1992**, *257*, 1677.
(23) Al-Ani, F. T.; Hughes, D. L.; Pickett, C. J. *J. Organomet. Chem*. **1986**, *307*, C31.
(24) Roussin, M. L. *Ann. Chim. Phys*. **1858**, *52*, 285.
(25) Goh, C.; Holm, R. H. *Inorg. Chim. Acta* **1998**, *270*, 46.

Table 1. Selected Bond Distances of the [$MoFe_3S_3$] Roussin-Type Compounds (Labels for the Atoms in the Compounds Are Shown in Figure 3)

bond	III	IV	IVa[a]	V	Va	VI	VIa	VII	VIII[b]
Mo1−O1	2.030(3)	2.037(4)	2.040(5)	2.041(4)	2.027(3)	2.095(4)	2.0684(18)	2.090(2)	2.098(8)
Mo1−O2	2.008(3)		2.045(4)	2.036(4)	2.042(3)	2.087(3)	2.0531(18)	2.068(3)	2.099(4)
Mo1−L		1.677(7)	1.691(4)	1.697(4)	1.685(3)	2.300(4)	2.364(2)	2.6706(12)	2.323(5)
Mo1−S1	2.3055(13)	2.428(2)	2.4204(19)	2.4372(16)	2.4186(12)	2.3270(13)	2.3179(6)	2.3278(9)	2.334(1)
Mo1−S2	2.2135(13)	2.595(2)	2.6145(18)	2.6368(16)	2.6198(11)	2.2800(12)	2.2651(6)	2.2979(9)	2.335(4)
Mo1−S3	2.3058(13)		2.4339(19)	2.4489(16)	2.4542(11)	2.3333(13)	2.3395(6)	2.3427(9)	2.327(4)
Fe1−S1	2.2512(13)	2.246(2)	2.251(2)	2.2502(18)	2.2465(12)	2.2066(13)	2.2455(7)	2.2512(10)	2.196(9)
Fe1−S2	2.3104(14)	2.2786(15)	2.304(2)	2.2888(17)	2.2790(12)	2.2949(13)	2.3244(7)	2.3176(10)	2.190(2)
Fe2−S1	2.2022(16)	2.220(2)	2.231(2)	2.2368(18)	2.2244(13)	2.1938(14)	2.2030(7)	2.2231(10)	2.292(9)
Fe2−S2	3.285	2.317(3)	2.310(2)	2.3133(17)	2.3059(11)	3.332	3.301	3.383	3.842
Fe2−S3	2.1739(14)		2.212(2)	2.2423(17)	2.2379(13)	2.1920(14)	2.1800(7)	2.1911(10)	2.285(6)
Fe3−S2	2.2965(13)		2.309(2)	2.2987(18)	2.2925(12)	2.2940(14)	2.2968(8)	2.3095(9)	2.181(4)
Fe3−S3	2.2014(14)		2.243(2)	2.2349(17)	2.2408(12)	2.2212(13)	2.2077(8)	2.2043(10)	2.208(2)
Fe1−P1	2.2621(14)	2.192(3)	2.224(2)	2.228(2)	2.2153(13)	2.2726(14)	2.2626(8)	2.2731(10)	2.253(5)
Fe3−P2	2.2570(14)		2.211(2)	2.2313(18)	2.2333(15)	2.2835(16)	2.2828(9)	2.2732(10)	2.26(2)
Fe1−C1	1.760(6)	1.752(9)	1.748(8)	1.787(8)	1.767(5)	1.794(5)	1.782(3)	1.781(4)	1.783(7)
Fe1−C2	1.778(6)	1.779(8)	1.754(8)	1.812(7)	1.789(5)	1.819(5)	1.787(3)	1.801(4)	
Fe2−C3(P3)	1.755(6)	2.239(4)	2.232(2)	1.799(7)	1.791(5)	1.784(6)	1.773(3)	1.774(4)	2.28(2)
Fe2−C4	1.769(6)	1.774(12)	1.765(9)	1.817(7)	1.794(5)	1.786(6)	1.770(3)	1.777(4)	1.802(7), 1.814(9)
Fe3−C5	1.787(6)		1.782(8)	1.795(7)	1.802(5)	1.791(5)	1.793(3)	1.809(4)	1.792(4)
Fe3−C6	1.806(6)		1.773(8)	1.800(7)	1.779(5)	1.800(5)	1.803(3)	1.808(4)	
Mo1−Fe1	2.8494(9)	3.723	3.735	3.776	3.712	2.7862(8)	2.8819(4)	2.8704(6)	2.651(1)
Mo1−Fe2	2.6793(9)	2.6917(16)	2.6790(13)	2.6633(10)	2.6710(7)	2.6689(8)	2.6737(4)	2.6820(6)	2.883(4)
Mo1−Fe3	2.7755(12)		3.724	3.742	3.787	2.8395(8)	2.7793(4)	2.7789(6)	2.66(1)
Fe1−Fe2	2.6248(11)	2.5746(14)	2.5669(16)	2.6360(13)	2.6204(9)	2.7030(10)	2.6155(5)	2.6414(7)	2.600(8)
Fe2−Fe3	2.7019(11)		2.5696(15)	2.6165(12)	2.6002(9)	2.6776(9)	2.6615(5)	2.7193(7)	2.59(2)
Fe1−Fe3	3.635	3.926	3.979	4.003	3.976	3.618	3.597	3.575	2.590(5)

[a] The structure has a crystallographic mirror plane through the Mo(1), the Fe(2), and S(2) atoms. [b] All bond distances are obtained by the average of each corresponding bond in two independent molecules in the unit cell.

Scheme 1. A Proposed Pathway toward the Synthesis of the [$MoFe_3S_3$] Roussin-Type Compounds

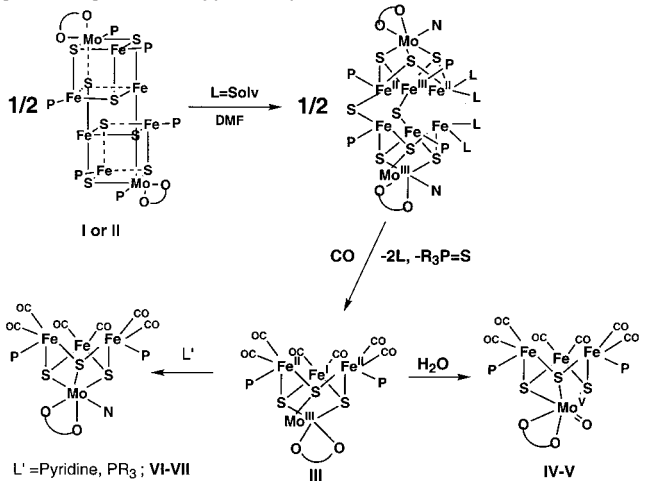

type clusters and of S═PR_3 (the latter has been isolated and characterized as a byproduct in these reactions). At present we are exploring synthetic conditions under which the hypothetical rearranged cluster, [$Mo_2Fe_6S_8(L)_4$] (Scheme 1), may be stabilized and subsequently converted to a $Mo_2Fe_6S_9$ cluster structurally similar to the FeMoco.

Rearrangement of **I** or **II** is not the only route to an FeMoco-like structure. Another class of clusters that are stoichiometrically analogous to FeMoco is the singly bridged[26] and doubly bridged[27] double-cubanes.[28] With core stoichiometries of Fe_8S_9 and $Mo_2Fe_6S_9$ these kinetically labile clusters also are likely sources of rearrangement products structurally analogous to the FeMoco of nitrogenase.

The previously reported **III** (Figure 2A) is the highest yield product in the reaction of **I** with CO (Scheme 1). This and a structurally analogous cluster with P^nPr_3 ligands afford the other products, **IV**−**VIII**. The oxo derivatives **IV**−**V** (Figure 2C) are obtained inadvertently in reactions of **III** with small amounts of O_2 impurity in the reaction media. One of these clusters, **V**, is obtained in 70% yield by the reaction[12] of **III** with Et_3NO. Addition of pyridine to **III** (Figure 2A) in CH_2Cl_2 is accompanied by a shift of the electronic absorption at 309 nm to one at 322 nm. The latter is a characteristic electronic absorption of **VI** (Figure 2B). Attempts to isolate **VI** from CH_2Cl_2 solution of **III**, containing an excess of pyridine, however, have not been successful and the only product obtained is crystalline **III**. Solutions of **III** in CH_2Cl_2 show partial decomposition and the infrared spectra of the vapors above these solutions show the presence of free CO. Upon prolonged standing these solutions eventually afford small quantities of the oxo cluster **IV**. The additional PEt_3 in **IV** probably derives from decomposed **III**. The origin of the oxygen atom, however, is not clear and may be due to minute trace amounts of O_2 in the inert atmosphere enclosure.

Generally, carbonyl ligands in the new clusters can be removed in solution under mild conditions at rates that depend on solvent polarity. In solvents such as DMF, NMF, and pyrolidinone all of the CO ligands can be removed within hours. The removal of CO from **VIa**, in CH_2Cl_2 solution, occurs readily by application of vacuum to this solution and **II** is obtained in 30% yield. The product was characterized completely and its X-ray crystal structure was re-determined. The oxidizing agent

(26) (a) Coucouvanis, D.; Challen, P. R.; Koo, S.-M.; Davis, W. M.; Burtler, W.; Dunham, R. W. *Inorg. Chem.* **1989**, *28*, 4181. (b) Coucouvanis, D.; Challen, P. R.; Koo, S.-M.; Davis, W. M.; Butler, W.; Dunham, W. R. *Inorg. Chem.* **1989**, *28*, 4181. (c) Huang, J.; Mukerjee, S.; Segal, B. M.; Akashi, H.; Zhou, J.; Holm, R. H. *J. Am. Chem. Soc.* **1997**, *119*, 8662.

(27) Demadis, K. D.; Chen, S.-J.; Coucouvanis, D. *Polyhedron* **1994**, *13*, 3147.

(28) Coucouvanis, D. *Acc. Chem. Res.* **1991**, *24*, 1.

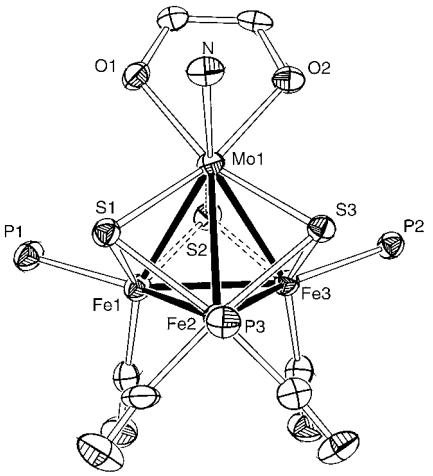

Figure 4. The crystallographic structure of the $(Cl_4\text{-cat})(Pyr)MoFe_3S_3(P^nPr_3)_3(CO)_4$ cluster (**VIIIa**).[12]

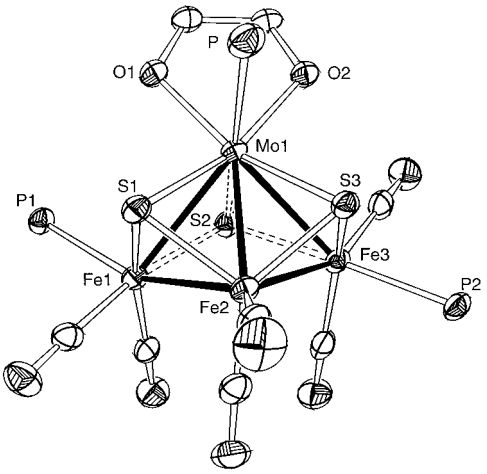

Figure 5. The crystallographic structure of the $(Cl_4\text{-cat})(P^nPr_3)MoFe_3S_3(P^nPr_3)_2(CO)_6$ (**VII**) cluster. The $(Cl_4\text{-cat})(Pyr)MoFe_3S_3(PEt_3)_2(CO)_6$ (**VI**) and the $(Cl_4\text{-cat})(Pyr)MoFe_3S_3(P^nPr_3)_2(CO)_6$ (**VIa**) clusters show the same core structure.

in this reaction at present is difficult to identify although it is possibly **VIa** serving as a sacrificial oxidant. The removal of CO ligands by evacuation is a known process[29] as is the oxidative decarbonylation process in oxidative coupling reactions.[30] Solution of **VIa** in CH_2Cl_2 or THF is extremely sensitive and fast formation of **Va** is observed. The addition of P^nPr_3 to **VIa** leads to instant generation of **VII**.

Structures. The structures of all clusters, obtained by the reactions of **I** and **II** with CO, contain as a common feature the distorted $MoFe_3S_3$ cuboidal core (Figure 2) where the Mo atom is bound by a bidentate Cl_4-cat ligand. With the exception of **III** (Figure 2A), which contains only the Cl_4-cat terminal ligand bound to the five-coordinate Mo atom, all other clusters contain an additional, monodentate, terminal ligand (oxo, pyridine, or trialkyl phosphine) bound to the Mo that shows a distorted octahedral coordination. The very short Mo−O bond, in **IV**−**Va** (Figure 2C), is considered a triple bond and the oxo-ligand serves as a six-electron donor. The terminal ligands (L) on the Fe atoms are the two electron donors, PR_3 and CO. The three iron atoms within the $MoFe_3S_3$ cores in all clusters are rearranged in triangular arrays. These arrays define isosceles Fe_3 triangles in all structures, except **VIII** (Figure 2D) where the three Fe atoms form a nearly equilateral triangle.

Clusters **III**−**VIII** can be subdivided into three groups depending on the number of terminal donor atoms and total number of valence electrons.

Ten Terminal-Donor Atom Tetranuclear Clusters with 60 Valence Electrons. The sole example of this type is cluster **VIII** (Figures 2D and 4), which contains seven Fe-bound terminal ligands in a distribution that gives two $(S)_2Fe(L)_2$ and one $(S)_2Fe(L)_3$ sites. The total count of valence electrons in this cluster is 60 e^-, which amounts to 15 e^- per metal atom and, according to bonding schemes used for organometallic clusters,[31] calls for complete M−M bonding in the distorted $MoFe_3$ tetrahedron. The bond length data for **VIII** (Table 1) accordingly show very short Fe−Fe and Mo−Fe distances with mean values of 2.592(5) and 2.73(9) Å, respectively. Two of the three Mo−Fe distances are significantly shorter (2.651(1) and 2.656(1) Å) than the third (Mo(1)−Fe(2) = 2.883(1) Å). These differences are very likely a direct consequence of the relative ligand crowding around the Fe(2) (three terminal ligands) by comparison to the Fe(1) and the Fe(2) (two terminal ligands each).

Ten or Eleven Terminal-Donor Atom Tetranuclear Clusters with 62 Valence Electrons. The nonoxo clusters **III** and **VI**−**VII** each contain eight, Fe-bound, terminal ligands and 62 valence electrons. In these (Figures 2A, 2B, and 5), the ligands are distributed to give two $(S)_2Fe(L)_3$ and one $(S)_2Fe(L)_2$ sites. The isosceles triangles of the Fe atoms in **VI**−**VII** show two short Fe−Fe distances with average values of 2.690, 2.638, and 2.680 Å in **VI**, **VIa**, and **VII**, respectively. The long Fe−Fe distances are found at 3.618, 3.597, and 3.575 Å. The mean Fe−Mo distances are 2.76(6), 2.78(7), and 2.78(9) Å. In all three of these structures the Mo(1)−Fe(2) distance is appreciably shorter (∼0.1 Å) than the other two and may be a consequence of the presence of only two terminal ligands around the Fe(2).

A comparison of the Fe−Fe distances between **VI**−**VII** and **VIII** shows a longer Fe(1)−Fe(3) distance in **VI**−**VII** by nearly one full angstrom relative to **VIII**. This long distance in **VI**−**VII** may be interpreted as due either to the greater number of valence electrons, which makes one of the metal−metal bonds unnecessary, or (less important) to the steric crowding around Fe(1) and Fe(3), each bound by three terminal ligands.

The relative importance of steric vs electronic effects in the length of the Fe−Fe distances at present is an open question. An answer to this question could be provided by a structure determination of the two-electron reduction product of **VIII** or the two-electron oxidation products of **VI**−**VII** (vide infra).

The M−M bonding in **III** (a cluster with 60 e^- if all the μ_3-S^{2-} ligands are considered to be 6e^- donors) should be similar to that in **VIII**. In fact it resembles more the bonding in the 62 e^- clusters with an isosceles triangle of Fe atoms and mean values of Mo−Fe and Fe−Fe distances of 2.77(6) and 2.99(40) Å, respectively. The data indicate that the S^{2-} ligand in the Mo(1)═S(2) (Figure 2A) short, multiple bond is best described as an eight-electron donor.

The Mo(1) in **III** is five coordinate and the coordination geometry can be described as square pyramidal with the S(2) ligand now serving as an axially coordinated ligand to the Mo

(29) Walters, M. A.; Dewan, J. C. *Inorg. Chem*. **1986**, *25*, 4889.
(30) Formation of $[Fe_4S_4(SPh)_4]^{2-}$ from $Fe_2S_2(CO)_6$ has been reported. Mayerle, J. J.; Denmark, S. E.; DePamphilis, B. V.; Ibers, J. A.; Holm, R. H. *J. Am. Chem. Soc*. **1975**, *97*, 1032.
(31) Pulliam, C. R.; Thoden, J. B.; Stacy, A. M.; Spencer, B.; Englert, M. H.; Dahl, L. F. *J. Am. Chem. Soc.* **1991**, *113*, 7398.

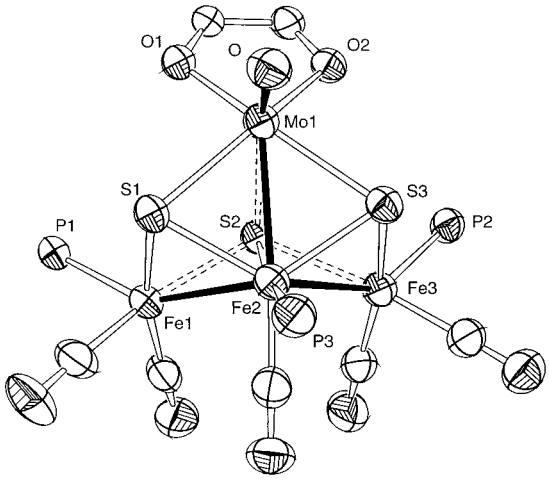

Figure 6. The crystallographic structure of the $(Cl_4\text{-cat})(O)MoFe_3S_3(P^nPr_3)_3(CO)_5$ (**IVa**) cluster. The $(Cl_4\text{-cat})(O)MoFe_3S_3(PEt_3)_3(CO)_5$ (**IV**), $(Cl_4\text{-cat})(O)MoFe_3S_3(PEt_3)_2(CO)_6$ (**V**), and $(Cl_4\text{-cat})(O)MoFe_3S_3(P^nPr_3)_2(CO)_6$ (**Va**) clusters show the same core structure.

atom which has O(1), O(2), S(1), and S(3) as equatorial ligands. The very short Mo(1)−S(2) bond at 2.213(1) Å is similar to Mo═S groups in other, known, thiomolybdenyl complexes.[32] The engagement of S(2) in the Mo═S multiple bond, as expected, has a pronounced effect in its function as a triply bridging ligand. The Fe(1)−S(2) and Fe(3)−S(2) distances at 2.310(1) and 2.296(1) Å are significantly longer than the other Fe-μ_3−S distances in **III** that range from 2.174(1) to 2.251(1) Å. In **III**, and also in **IV**−**Va** (vide infra), the coordination around the Mo atoms illustrates the pronounced structural importance of the, potentially axial, Mo═E group (E = O, S) in promoting square pyramidal or distorted square pyramidal Mo-centered substructures.

Eleven Terminal-Donor Atom Tetranuclear Clusters with 66 Valence Electrons. In the oxo clusters **IV**−**Va** (Figures 2C and 6) with 66 valence electrons, the M−M distances are elongated further. The differences between the short and the long Fe−Fe distances are approximately 1.4 Å, and greater than those found in the **III** and **VI**−**VII** clusters (approximately 1.0 Å, Table 2).

The Mo−Fe distances in **IV** to **Va** are separated into two groups: long Mo(1)−Fe(1) and Mo(1)−Fe(3) distances (3.712−3.787 Å range) and short Mo(1)−Fe(2) distances (2.663(1)−2.679(1) Å range). The nonoxo clusters **III** and **VI**−**VIII** (Table 1) do not show a similar pronounced disparity in the Mo−Fe distances which fall within the range 2.669(1)−2.8814(4) Å.

The Mo═O bonds in **IV**−**Va** are found within the range from 1.677(7) to 1.697(4) Å and are similar to those observed in other molybdenyl complexes.[32] The trans effect of the Mo═O group is illustrated in the long Mo(1)−S(2) bonds in **IV**−**Va** that range from 2.597(2) to 2.637(1) Å. They are considerably longer than the equatorial Mo(1)−S(1) and Mo(1)−S(3) bonds (2.419(1)−2.449(1) Å range). The structural data for the oxo clusters, **IV**−**Va** (Table 1), indicate that the coordination geometry of the Mo atoms is best described as distorted six-coordinate with a square pyramidal unit (axial Mo═O group and equatorial O(1), O(2), S(1), and S(3) ligands) coordinated by a distant sulfido ligand, S(2), trans to the Mo═O group. In **IV**−**Va**, one of the S^{2-} ligands, S(2), is four-coordinate and considered a μ_4-ligand (and therefore contributes eight electrons) with the S(2)−Mo-(1) distance at 2.595(2) Å, and S(2)−Fe(1), S(2)−Fe(2), and S(2)−Fe(3), distances of 2.279(1), 2.317(3), and 2.279(1) Å. The Fe(1,3)−S(2) distances are significantly longer than the remaining Fe(1,2,3)−S(1,3) distances that span the range from 2.212 to 2.251 Å with a mean value of 2.237(3) Å.

Possible M−M Bonding in the FeMoco. Collectively, the Mo−Fe and Fe−Fe distances in clusters with 60 e^- (**VIII**), 62e^- (**VI**−**VII**), and 66e^- (**IV**−**Va**) are 2.592(5) and 2.73(9) Å, 2.77-(2) and 2.98(16) Å, and 3.38(19) and 3.05(24) Å. Qualitatively, these changes indicate that from **VIII** to **VI**−**VII** to **IV**−**Va**, electrons are added primarily to Fe−Fe and then Mo−Fe antibonding orbitals. *It appears that as the total number of valence electrons decreases, the clusters undergo structural changes that allow for electron sharing via M−M bond formation.* In addition, available lone pairs on bridging sulfido ligands may be committed to multiple M−S bonding within the clusters' cores (as in **III**).

This ability of the μ-S^{2-} ligands to contribute additional pairs of electrons to the valence electron count may be important to the bonding within the nitrogenase cofactor where the total electron count is insufficient to support the M_8S_9 core with only single M−M bonds. In the FeMoco, assuming a formal $Mo^{IV}Fe^{III}_3Fe^{II}_4$ metal ensemble,[33] there are three μ_2-S^{2-} and six μ_3-S^{2-}ligands, three terminal negative 2e^- ligands (homocitrate and Cys), and a neutral 2 e^- ligand (His). The total number of valence electrons in the $MoFe_7S_9(L)_4$ monoanion is 97. This small number of electrons suggests that multiple M−M bonding and M═S bonding may be needed to support the structure of the cofactor and the coordinatively unsaturated FeS_3 units. An examination of structural data for the FeMoco (Figure 1) shows a large number of not only short Fe−Fe and Fe−Mo distance ranges for Fe−Fe distances (2.62−2.67 Å[1c] and 2.52−2.62 Å)[1b] but also of short Mo−S and Fe−S bonds (range for Fe−S bonds: 2.21−2.26 Å). Admittedly, the large standard deviation in these bonds (0.01−0.02 Å) poses doubts as to their significance. The consistent similarity in the values of chemically equivalent bonds, however, is more reliable and may be a better indicator of significance. The similarity of **VIII** to one of the cuboidal subunits in the FeMoco (Figure 3B) suggests that decarbonylation of **VIII** in the presence of S^{2-} may be a route to a cofactor-like structure. Whether such a structure will be stable enough to be isolated remains to be established.

Mössbauer Spectroscopy. The ^{57}Fe Mössbauer spectra of all clusters (**III**−**VIII**) were simulated by using three quadrupole doublets of equal intensity. These doublets[34] are characterized by small values for the isomer shifts and quadrupole splittings by comparison to other biological[35] or synthetic[19,36] Fe/S clusters. Tentative assignments of the doublets to the various Fe sites in each structure are based on ligand environment and coordination geometry.

The oxidation states for the Fe centers, as indicated in Table 2, have been chosen between two possible, realistic, allocations of oxidation states that give rise to the $[MoFe_3]^{8+}$ cores in **III** and **VI**−**VIII** and the $[MoFe_3]^{10+}$ cores in **IV** and **V**.

(32) Coucouvanis, D. *Adv. Inorg. Chem.* **1998**, *45*, 1.
(33) Yoo, S. J.; Angove, H. C.; Papaefthymiou, V.; Burgess, B. K.; Münck, E. *J. Am. Chem. Soc.* **2000**, *122*, 4926.
(34) Mossbauer spectra and cyclic voltammetry traces have been deposited as Supporting Information.
(35) Beinert, H.; Holm, R. H.; Munck, E. *Science* **1997**, *277*, 653.
(36) Goh, C.; Segal, B. M.; Huang, J.; Long, J. R.; Holm, R. H. *J. Am. Chem. Soc.* **1996**, *118*, 11844.

Table 2. Mössbauer Parameters for the $(Cl_4\text{-cat})MoFe_3S_3(PEt_3)_2(CO)_6$ (**III**), $(Cl_4\text{-cat})(O)MoFe_3S_3(PEt_3)_3(CO)_5$ (**IV**), $(Cl_4\text{-cat})Mo(O)Fe_3S_3(PEt_3)_2(CO)_6$ (**V**), $(Cl_4\text{-cat})(Pyr)MoFe_3S_3(PEt_3)_2(CO)_6$ (**VI**), $(Cl_4\text{-cat})(P^nPr_3)MoFe_3S_3(P^nPr_3)_2(CO)_6$ (**VII**), and $(Cl_4\text{-cat})(Pyr)MoFe_3S_3(P^nPr_3)_3(CO)_4$ (**VIII**) Clusters in Zero Applied Magnetic Field

compd	Fe center	geometry	ligands	δ, ΔE_Q (mm/s)	av δ(mm/s)
III	1	square pyramid	$S_2P(CO)_2$	0.053, 1.080	
	2	trigonal pyramid	$S_2(CO)_2$	0.100, 0.358	0.078
	3	trigonal bipyramid	$S_2P(CO)_2$	0.074, 1.440	
IV	1	square pyramid	$S_2P(CO)_2$	0.010, 0.788	
	2	trigonal bipyramid	S_3PCO	0.121, 0.307	0.059
	3	square pyramid	$S_2P(CO)_2$	0.045, 0.858	
V	1	square pyramid	$S_2P(CO)_2$	0.014, 0.795	
	2	trigonal bipyramid	$S_3(CO)_2$	0.087, 0.241	0.044
	3	square pyramid	$S_2P(CO)_2$	0.032, 0.831	
VI	1	trigonal bipyramid	$S_2P(CO)_2$	0.108, 1.297	
	2	trigonal pyramid	$S_2(CO)_2$	0.120, 0.307	0.108
	3	trigonal bipyramid	$S_2P(CO)_2$	0.095, 1.452	
VII	1	square pyramid	$S_2P(CO)_2$	0.128, 1.103	
	2	trigonal pyramid	$S_2(CO)_2$	0.111, 0.368	0.128
	3	trigonal bipyramid	$S_2P(CO)_2$	0.135, 1.402	
VIII	1	square pyramid	$S_2P(CO)_2$	0.121, 0.349	
	2	trigonal pyramid	S_2PCO	0.126, 1.063	0.124
	3	trigonal pyramid	S_2PCO	0.125, 1.403	

The former of these can be described in terms of $Mo^{III}Fe^{II}_2Fe^{I}$ or $Mo^{IV}Fe^{I}_2Fe^{II}$. The latter could be either $Mo^{V}Fe^{II}_2Fe^{I}$ or $Mo^{VI}Fe^{I}_2Fe^{II}$. The $(S)_3(O)_3$ coordination sphere in **IV** or **V** is assigned to the larger ionic radius Mo^{V} rather than Mo^{VI} and consequently the Fe oxidation states in all neutral clusters are considered as $Fe^{II}_2Fe^{I}$.

The low values of the isomer shifts in all clusters are due mainly to the π accepting nature of the CO ligands and to a lesser extent that of the PR_3 ligands. Back-bonding from the Fe d orbitals to the ligands reduces the 3d electron density on the Fe atoms and indirectly reduces the screening of s electron density from the ^{57}Fe nucleus. This results in the observed small values of the isomer shifts.

The δ values for **III**−**VIII** occur in the range 0.01 to 0.15 mm/s, which also is the "normal" range for other organo-iron compounds.[37] Mössbauer spectra with δ values in the above range are available for a number of six-coordinate mononuclear Fe−(CO, PR_3) or Fe−(NO, CO) complexes.[38] Similar Mössbauer parameters also have been found for oligonuclear compounds that contain bridging S^{2-} ligands, and are more appropriately relevant to the clusters in this paper. Included among these compounds are the $Fe^{II}_2S_2(CO)_6$ dimer,[39] the $[MoFe^{II}_2S_2(CO)_8(S_2(NEt_2))^-]$,[40] and the $[(NNR_2)_2(PR'_3)MoFe^{I}_2S_2(CO)_8\ (S_2(NEt_2))^-]$[41] clusters. For the latter, δ values and ΔE_Q values were reported, respectively, as 0.068 mm/s, 1.088 mm/s (at 77 K);[39] 0.008 mm/s, 0.965 mm/s;[40] and 0.033−0.064 mm/s, 0.707−0.800 mm/s.[41] The only examples of organometallic-like centers in biological systems are found in the hydrogenases.[42] The H-cluster in [Fe]-hydrogenase has an Fe center with pentacoordinate and hexacoordinate iron sites and S^{2-}, CO, and CN^- coordination. The Mössbauer spectra of these low-spin Fe^{II} sites show δ and ΔE_Q values of 0.08 and 0.85 mm/s. A synthetic analogue for the Fe component of the active site of [Ni,Fe]-hydrogenase has been reported.[43] This compound has octahedrally coordinated Fe(II) with three S donors and one CO as equatorial ligands and CN^- and PR_3 as axial ligands. The Mössbauer spectrum of this compound has δ and ΔE_Q values of 0.15 mm/s and 0.91 mm/se, respectively. The unprecedented structural motif of the $[MoFe_3S_3]$ centers makes assignment of the Mössbauer absorptions to specific sites difficult. *Distinguishing formal oxidation states (i.e. Fe^{I} from Fe^{II}) in the presence of CO ligands and M−M bonding is speculative and the proposed assignments (Table 2) are based mainly on ligand environment and coordination geometry, not taking into account the M−M bonds.*

An examination of the data shown in Table 2 leads to the general conclusion that a larger number of valence electrons is associated with smaller average values of δ. Thus **IV** and **V** with 66 valence electrons show δ values at 0.06 and 0.04 mm/s, respectively. The **III** and **VI**−**VIII** clusters with 60 or 62 electrons display average isomer shifts in the range 0.08−0.13 mm/s.

Electrochemistry. The electrochemistry of the $MoFe_3S_3$ clusters (Table 3) is dominated by reversible or quasireversible reductions expected for these electron-deficient clusters. For **III**−**VIII** in dichloromethane or 1,2-dichloroethane, the first reduction occurs between −0.5 and − 0.8 V. Addition of electrons is expected to result in fewer metal−metal bonds and may or may not be accompanied by pronounced structural changes. The reversible nature of most of these reductions indicates that addition of electrons to the clusters does not result in cluster decomposition or radical structural changes. The two-electron reduction of the 60 e^- **VIII** most likely leads to a 62 e^- cluster isoelectronic to **VI**. Whether elongation of one M−M bond follows this reduction and steric crowding determines the metal−metal bond that undergoes this elongation remains to be established. The two-electron reversible reduction of **IV**[34] similarly may result in a reduction in the M−M bonding. The

(37) (a) *Chemical Mössbauer Spectroscopy;* Herber, R. H., Ed.; Plenum press: New York, 1985; pp 6−25. (b) *Mössbauer Spectroscopy;* Greenwood, N. N., Gibb, T. C., Eds.; Chapman and Hall: London, 1971.
(38) (a) Bancroft, G. M.; Libbey, E. T. *J. Chem. Soc., Dalton* **1973**, 2103. (b) Libbey, E. T.; Bancroft, G. M. *J. Chem. Soc., Dalton* **1974**, 87. (c) Sipio, L. D.; Calogero, S.; Albertin, G.; Orio, A. A. *J. Organomet. Chem.* **1975**, 257. (d) McAuliffe, C. A.; Niven, I. E.; Parish, R. V. *J. Chem. Soc., Dalton* **1976**, 2477. (e) Sams, J. R.; Scott, J. C. *J. Chem. Soc., Dalton* **1974**, 2265. (f) Carroll, W. E.; Deeney, F. A.; Delaney, J. A.; Lalor, F. J. *J. Chem. Soc., Dalton* **1973**, 718.
(39) Dilworth, J. R.; Morton, S.; O'Connor, M.; Silver, J. *Inorg. Chim. Acta* **1987**, *127*, 91.
(40) Zhuang, B.; Chem, P.; Huang, L.; Lu, J. *Polyhedron* **1992**, *11*, 127.
(41) Bishop, P. T.; Dilworth, J. R.; Morton, S.; Zubieta, J. A. *J. Organomet. Chem.* **1988**, *341*, 373.
(42) Popescu, C. V.; Münck, E. *J. Am. Chem. Soc.* **1999**, *121*, 7877.
(43) Hsu, H.-F.; Koch, S. A.; Popescu, C. V.; Münck, E. *J. Am. Chem. Soc.* **1997**, *119*, 8371.

Table 3. Cyclic Voltammetry Measurements of the $[MoFe_3S_3]$ Roussin-Type Compound[a]

compd	solvent	reduction, mV	oxidation, mV
I	CH_2Cl_2	−890 (rev)	50 (qr)
II	CH_2ClCH_2Cl	−248 (qr), −547 (qr), −911 (qr)	200 (qr)
III	DMF	−222 (rev), −574 (irr), −676 (rev), −922 (irr)	214 (irr), 520 (rev), 756 (irr)
III	CH_2Cl_2	−756 (qr), −888 (qr)	846 (irr)
IV	CH_2Cl_2	−677 (rev)	300 (irr), 500 (irr), 720 (irr)
IV	CH_2ClCH_2Cl	−524 (rev), −656 (rev), −1230 (irr)	760 (irr)
V	CH_2ClCH_2Cl	−639 (rev), −1288 (rev)	980 (rev)
VIa	CH_2ClCH_2Cl	−800 (rev)	752 (irr)
VIII	CH_2ClCH_2Cl	−798 (rev), −1066 (rev)	400 (irr), 622 (irr)

[a] For the all experiments, the reference electrode was Ag/AgCl and the electrolyte was 0.1 M of $^nBu_4NPF_6$. irr = irreversible, rev = reversible, qr = quasi-reversible. The scan rates for the compounds, except compounds **I** and **III**, were 100 mV/s. The cyclic voltammetry data for **I** and **III** have been reported in refs 13 and 11, respectively.

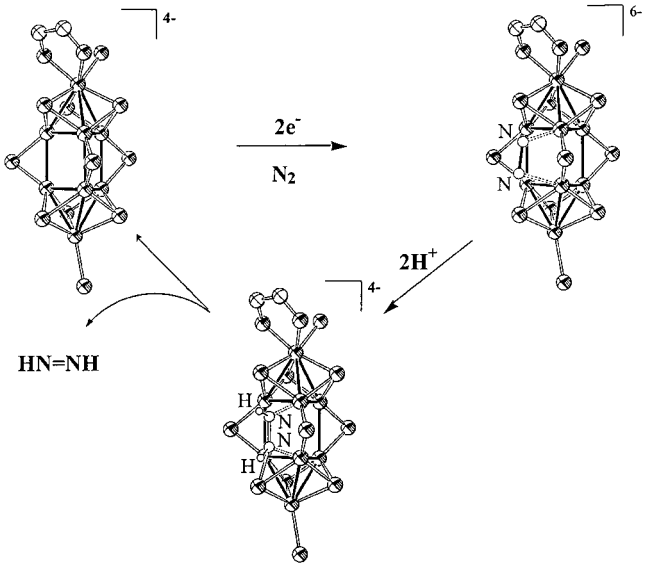

Figure 7. A proposed mechanism for the binding and activation of dinitrogen on the FeMoco, taking advantage of M−M bonds.

lack of sufficient amounts of either **VIII** or **IV** at this time precludes the chemical reduction of these clusters. However, their reduction and structure determination of the products will provide important insights regarding the structural changes that accompany reduction of this type of cluster.

The structure of the FeMoco, as presently known, is three electrons oxidized relative to the state at which the activation and reduction of N_2 occurs. The electrochemical characterization of the isolated FeMoco has shown a quasireversible one-electron reduction from the oxidized form to the semireduced form occurred at −0.33V vs NHE (−0.56V vs Ag/AgCl), and a second quasireversible reduction to the reduced form of FeMoco at −1.0V vs NHE (−1.23 V vs Ag/AgCl).[44] The binding of CO molecule to the isolated FeMoco also has been observed after this second reduction (later shown to be a two-electron reduction) of the isolated FeMoco, in the presence of gaseous CO.[45]

The possibility that a multielectron reduction of the highly electron deficient cofactor may lead to a significant structural change of this molecule suggests a possible mechanism for the activation and reduction of N_2. In this proposed mechanism (Figure 7), an Fe−Fe bond (intra- or inter-subunit) is a site where the two electrons are deposited into the reduced form of FeMoco. Opening of this bond generates a site where the N_2 can be accommodated (bridged or end-on mode) and activated (by protonation or H-bonding). Following activation the two electrons are delivered to the N_2 to generate diazene and reform the Fe−Fe bond. Similar mechanisms for the reduction of N_2 on the Fe_6 central unit in the FeMoco have been proposed.[46] These mechanisms do not consider the possible involvement of M−M bonding in the storage and delivery of electrons. *The storage of reducing equivalents into M−M bonds and their use in the reduction of substrates may account for the presence of apparently extensive M−M bonding in the nitrogenase cofactor.*

Acknowledgment. The authors acknowledge the support of this work by a grant from the National Institutes of Health (GM 33080).

Supporting Information Available: Tables giving structure determination summary, atomic coordinates, bond lengths and bond angles, and anisotropic thermal parameters for $(Cl_4\text{-cat})(O)MoFe_3S_3(P^nPr_3)_3(CO)_5$ (**IVa**), $(Cl_4\text{-cat})(O)MoFe_3S_3(P^nPr_3)_2(CO)_6$ (**Va**), $(Cl_4\text{-cat})(Pyr)MoFe_3S_3(P^nPr_3)_2(CO)_6$ (**VIa**), and $(Cl_4\text{-cat})(P^nPr_3)MoFe_3S_3(P^nPr_3)_2(CO)_6]$ (**VII**) (PDF). This material is available free of charge via the Internet at http://pubs.acs.org. For the remaining structures, crystallographic data have already been deposited.[11,12]

JA0110832

(44) Schultz, F. A.; Gheller, S. F.; Burgess, B. K.; Lough, S.; Newton, W. E. *J. Am. Chem. Soc.* **1985**, *107*, 5364.
(45) Ibrahim, S. K.; Vincent, K.; Gormal, C. A.; Smith, B. E.; Best, S. P.; Pickett, C. J. *Chem. Commun.* **1999**, 1019.
(46) (a) Dance, I. G. *Aust. J. Chem.* **1994**, *47*, 979. (b) Sellman, D.; Fürsattel, A.; Sutter, J. Coord. Chem. Rev. **2000**, *200−202*, 545.